letters to nature

31. Benner, R. & Strom, M. A critical evaluation of the analytical blank associated with DOC measurements by high-temperature catalytic oxidation. *Mar. Chem.* **41**, 153–160 (1993).
32. Hedges, J. I. & Stern, J. H. Carbon and nitrogen determinations of carbonate-containing solids. *Limnol. Oceanogr.* **29**, 657–663 (1983).

Variability of the North Atlantic thermohaline circulation during the last interglacial period

Jess F. Adkins*§, **Edward A. Boyle***, **Lloyd Keigwin**† & **Elsa Cortijo**‡

* *Department of Earth Atmosphere and Planetary Sciences, Massachusets Institute of Technology, Cambridge, Massachusetts 02139, USA*
† *Woods Hole Oceanographic Institution, Woods Hole, Massachusetts 02543, USA*
‡ *Centre des Faibles Radioactivitis, Laboratoire mixte CNRS-CEA 91198, Gif-sur-Yvette Cedex, France*

Studies of natural climate variability are essential for evaluating its future evolution. Greenland ice cores suggest that the modern warm period (the Holocene) has been relatively stable for the past 9,000 years[1,2]. Much less is known about other warm interglacial periods, which comprise less than 10% of the climate record during the past 2.5 million years[3–7]. Here we present high-resolution ocean sediment records of surface and deep-water variables from the Bermuda Rise spanning the last interglacial period, about 118,000–127,000 years ago. In general, deep-water chemical changes are coincident with transitions in surface climate at this site. The records do not show any substantial fluctuations relative to the much higher variability observed during the preceding and subsequent cool climates. The relatively stable interglacial period begins and ends with abrupt changes in deep-water flow. We estimate, using [230]Th measurements to constrain the chronology, that transitions occur in less than 400 years.

Early results from the GRIP ice core project suggested large climatic changes during the last interglacial[2,8], taken here as roughly equivalent to marine oxygen isotopic stage 5e and the Eemian interglacial on land[9]. Because of structural studies of the ice sheet's bedding[10], comparison with the GISP2 record[1] and studies of the $\delta^{18}O$ of atmospheric oxygen[11], the largest of these apparent climatic instabilities now appear to be artefacts of ice disturbance near the bottom of the core. Nevertheless, the Greenland ice sheet data highlighted how little is known of the climate stability of warm climate periods such as stage 5e, inspiring detailed climate studies on land[6,7] and in marine records[3–5,12,13]. As part of the IMAGES coring program, we raised a 52.7-m-long core (MD95-2036, 33° 41.444′N, 57° 34.548′W, 4,462 m water depth) from the Bermuda Rise, a North Atlantic sediment drift deposit. This core has a continuous record of sedimentation from the Last Glacial Maximum back through the penultimate glaciation (Fig. 1). Visible light reflectance data from the core (a proxy for %CaCO$_3$) show that we have collected a record that includes all of the major interstadials from 5 to 21 that have been previously identified in Greenland ice cores. Extremely high deposition rates (10–200 cm kyr^{-1}) and penetration through the marine isotope stage 6 provide a unique archive of the ocean's behaviour. As has been previously reported[14], this site is a sensitive indicator of basin scale deep-water chemical variability. Here we present results on the foraminiferal chemistry

and [230]Th-based clay and carbonate accumulation rates in this core from the depth interval from 42 to 44 m, including marine stages 5e and 5d. To achieve the highest possible temporal resolution, the core was sampled at 1-cm intervals, taking care to avoid extraneous material from burrow structures. Although this sample spacing may seem very fine, it is important to note that bulk density data show that an original depth interval of ~2.4 cm has been compacted to 1 cm.

Several geochemical tracers are used here (Fig. 2). $\delta^{18}O$ measurements of the planktonic foraminiferan *Globigerinoides ruber* reflect a mixture of the global ice volume signature and local surface temperature and salinity conditions. Similarly, benthic $\delta^{18}O$ data reflect deep-water temperatures and the $\delta^{18}O$ value of deep water at this site (determined by global ice volume and deep water hydrography). For the global deep ocean, the $\delta^{18}O$ variation between glacial and interglacial extrema is usually considered to be about two-thirds ice volume and about one-third temperature[15] (although one study argues for a larger role for temperature in the South Atlantic[16]). Cd/Ca ratios were obtained from the benthic foraminiferan *Nutallides umbonifera*. These data reflect the relative mixture of nutrient-depleted waters of a northern origin (low Cd/Ca) with nutrient-enriched source waters of a southern origin (high Cd/Ca)[14,17,18]. The foraminiferal dissolution index responds to the corrosiveness of bottom waters to CaCO$_3$. Because *Cibicidoides wuellerstorfi* abundance is extremely low in several zones, the benthic $\delta^{13}C$ record is incomplete. These $\delta^{13}C$ data are given in the Supplementary Information, but for deep-water chemical variability we depend instead on the more complete Cd/Ca data[19]. Spectrophotometric reflectance data from the raw sediment were obtained immediately on core splitting[20]; these data are summarized with CIE (Commission Internationale de l'Éclairage) 'L' (lightness) and 'a' (red-to-yellow colour balance) indices. Lightness reflects the relative abundance of white CaCO$_3$ and (typically) darker non-carbonate aluminosilicate material, and the red-to-yellow colour balance reflects the abundance of haematite-rich sediment from the Maritime Provinces of Canada[21,22]. Finally, clay and carbonate fluxes were calculated from %CaCO$_3$ measurements and from excess [230]Th° (where ° stands for decay-corrected) determined, on every other sample, by inductively coupled plasma mass spectrometry (ICP-MS). This calculation is based on the precisely known production rate of [230]Th in the water column by dissolved uranium (in flux units of d.p.m. cm^{-2} kyr^{-1}) and the efficient removal of this [230]Th to the underlying sediment. On a basin-wide scale, the concentration of [230]Th in surface sediments (in units of d.p.m. g^{-1}) is inversely proportional to the total sediment input to the basin (in flux units of g cm^{-2} kyr^{-1}). After accounting for decay since deposition at the surface, down-core accumulation rates of individual sediment components can then be calculated by dividing the [230]Th° expected by the concentration measured and multiplying by the component concentration[23–25].

An age model for the interval studied was developed from $\delta^{18}O$ stratigraphy and [230]Th-constrained flux variations. Two time control points are taken from the Martinson *et al.*[26] orbitally tuned benthic isotope stack: the beginning of the 5/6 transition (4,380 cm = 131 kyr BP) and the 5d/5e transition (4,280 cm = 114 kyr BP). Previous work at this site established that the sediment composition is a balance between biogenic carbonate (and a small amount of atmospheric dust) falling out of the ocean surface and aluminosilicates from the continental margin transported into the interior of the basin by deep-sea currents[27]. The sedimentation rate at this site is enhanced by lateral sediment focusing, where freshly deposited material is removed from some areas of the seafloor by deep-sea currents and then transported to this site. Low-resolution data from the Holocene[27] and our unpublished studies based on detailed ^{14}C dates at this site for the past 3,000 yr indicate that the basin-wide clay flux and the local focusing factor are correlated, probably linked by seafloor circulation characteristics that control both margin erosion and lateral transport. The [230]Th focusing factor

(F) is the ratio of total excess ^{230}Th° found at a site divided by the amount expected from production in the overlying water column. Normally F is calculated by integrated excess ^{230}Th° measured between two well-dated sediment horizons and dividing by the amount produced during that time interval. Here, instead, we use %CaCO$_3$ as a proxy for variations in F and use the excess ^{230}Th° measurements to calculate ages in 2-cm intervals. This process allows us to adjust our age model for the changes in accumulation rate between stable-isotope age control points.

We assume that there is a linear relation between F and %CaCO$_3$ during stage 5e (as seen in the Holocene and deglaciation data) and that the slope is as close to the Holocene value as it can be subject to the constraints below. The slope ($m = -6.7$) and intercept ($b = 56\%$) of this relation are chosen so that

$$\int_{t=114\,\text{kyr}}^{131\,\text{kyr}} F(t)\mathrm{d}t = F_{\text{average}}(131\,\text{kyr} - 114\,\text{kyr})$$

In practice, we evaluate the integral at our sampling resolution of 2 cm and use our proxy generated F values to calculate the ages (Δt) between these depths. In this way, the age model is improved from an assumption of constant sedimentation between benthic isotope control points:

$$\sum \frac{^{230}\text{Th}°_{\text{ex}}\rho\Delta z}{\beta(\text{water depth})} = F_{\text{average}}T = \sum(m\%\text{CaCO}_3 + b)\Delta t$$

$$\sum \Delta t = T$$

$$F \geqslant 1$$

Here the summation is done over the depth range for which there are ^{230}Th°$_{\text{ex}}$ measurements. T is the time interval, from benthic isotope control points, of this depth range; β is the water-depth-dependent ^{230}Th production rate constant; and ρ is the dry bulk density. The slope and intercept of the first equation are chosen as described above and such that F is always greater than one. This constraint of no winnowing (consistent with all measured F from this site) coupled with different Holocene and stage 5e %CaCO$_3$ maxima causes the F–%CaCO$_3$ relationship to be different for the two time periods (Holocene values: $b = 35\%$, $m = -0.5$). These differences are inconsequential in relation to the conclusions discussed below. If we assumed the extreme case of constant F between our two stable isotope age control points, the age of the terminal stage 5e event would increase by 2 kyr and the duration of this event would increase from 410 to 830 yr. Above the zone with ^{230}Th data, a constant accumulation rate of 11 cm kyr^{-1} is assumed, to be consistent with sedimentation rates immediately below and inferred ages of isotopic stages 5a and 5c (as determined from the optical reflectance stratigraphy).

At the site of MD95-2036, Cd data from the four oldest samples indicate that a significant component of low-nutrient North Atlantic Deep Water (NADW) was present at this site during early termination II (Fig. 2), although Cd is somewhat higher (lower %NADW)

than seen during stage 5e or the Holocene. The largest signal in the benthic Cd data show that stage 5e is preceded by an abrupt cessation of NADW supply to this site lasting about 1,500 yr, coeval with the Glacial to Interglacial transition (Fig. 2). This may be the same event observed by Oppo *et al.*[13] in a core shallower and farther to the north. A similar event has also been reported at this site for early deglaciation near the end of isotope stage 2 (refs 14, 19). All of these events may be coeval with 'Heinrich' ice rafting events. At the end of the termination II event, Cd values are low and similar to Holocene values,[14] and benthic δ^{18}O attains values characteristic of full interglacial conditions. The bottom-water saturation state, as indicated by the fragmentation index, closely follows the Cd/Ca record, possibly with a slight time lag. This fragmentation record supports Cd/Ca evidence for NADW variability at this site. The clay flux peaks early on termination II, just preceding NADW disappearance from this site. This peak clay flux probably reflects higher sediment influx from Canada during glacial disintegration. The fine-grained aluminosilicates from this eroded material are first deposited on the Laurentian Fan,[22] scoured by the western boundary current, and then laterally transported on to the Bermuda Rise.[28] The coincident enhanced reddish colour of the sediment—signifying hematite from the Canadian Maritimes—supports this interpretation. The data from the 5/6 transition show that the steepest change in δ^{18}O and the NADW retreat from this site are synchronous, but also show that clay flux precedes this transition and the deep-water change.

Planktonic and benthic δ^{18}O are well correlated throughout stages 5e and 5d; both attain full interglacial values at ~129 kyr BP and remain relatively constant for the next 8,000 years. Fine-scale structure in the planktonic record shows three zones of δ^{18}O variability: (1) values of about -0.79 ± 0.16‰, with a slight decreasing trend during stage 5e; (2) more scattered values of ~0.25 ± 21‰ during stage 5d; and (3) generally increasing values on the 5e to 5d transition. The climatic record at this site does not show a switch towards glacial conditions until there is a chemical change in the deep waters. Late within isotope stage 5e (~118 kyr BP), there is a rapid shift in oceanic conditions in the western North Atlantic that has not been previously documented. Within a 2-cm interval, %CaCO$_3$ drops abruptly, and clay flux, Cd/Ca, percentage fragmentation and red/yellow colour balance all rise equally abruptly. These data indicate a coincident increase both in the proportion of southern source waters and the recirculation-derived clay supply. Immediately afterwards, benthic δ^{18}O begins a steady increase into marine isotope stage 5d. The rise in Cd/Ca, carbonate flux and red-to-yellow colour balance are short-lived, occurring over <8 cm (~400 yr), whereas the clay flux decreases more gradually. Surface tracers (*G. ruber* δ^{18}O and CaCO$_3$ flux) are coincident with deep tracers (Cd/Ca and clay flux) but with a smaller amplitude. The rapid deep and surface hydrographic changes found in this core mark the end of the peak interglacial and the beginning of climate deterioration towards the semi-glacial
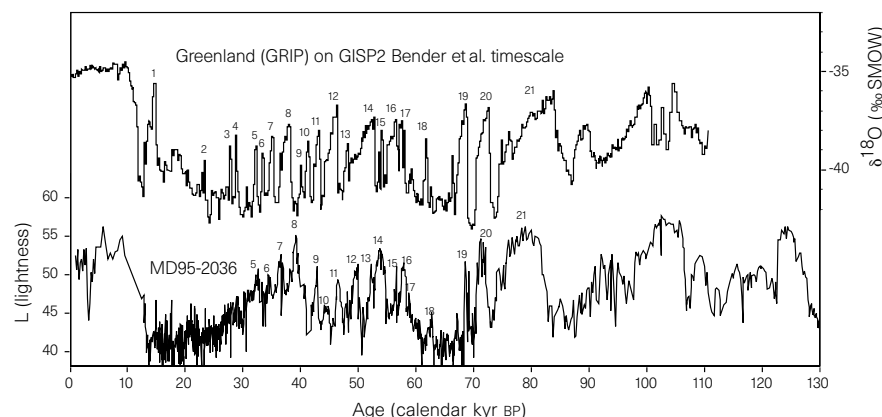

Figure 1 Bermuda Rise sediment grey scale compared with GRIP ice core δ^{18}O. Lightness data were collected for MD95-2036 as described in the text. Ice core δ^{18}O data are from the GRIP ice core project.[2] The age model is obtained by correlating the GISP II δ^{18}O–age record with the GRIP δ^{18}O–depth record. Numbered intervals correspond to interstadial events identified in the ice core record. All events from 5 to 21 are identifiable in the marine cores, indicating a continuous record of climate up to the penultimate glaciation. SMOW, standard mean ocean water.

stage 5d. Before and immediately after this event, signalling the impending end of stage 5e, deep-water chemistry is similar to modern NADW. As climate deteriorates into stage 5d, the deep circulation becomes more variable (Cd/Ca$_{5d}$ = 0.099 ± 0.021 and Cd/Ca$_{5e}$ = 0.071 ± 0.010).

Data from the Bermuda Rise reveal several important features of the climate stability during stage 5e and the penultimate glacial transition. By augmenting the δ^{18}O stratigraphy with high-resolution ^{230}Th profiling, we can place our records on a more refined absolute age scale. During stage 5e, we find climate stability lasting ~8,000 yr in both surface and deep waters at the Bermuda Rise. Although there are significant events during this warm period, the variance of our climate tracers during stage 5e is smaller than in the following cold stage and the preceding glacial transition. This stability is punctuated, at the end of the last interglacial plateau, by an abrupt event that begins the transition to a harsher climate. Over ~400 yr, Cd/Ca ratios, clay flux, percentage fragmentation and the red/yellow colour balance all show a synchronous switch to bottom waters that have a higher proportion of southern source component. It is this deep-water event that marks the descent into isotopic stage 5d. Our data indicate that climatic shifts are strongly related to deep-water reorganizations[12,13] and that these changes can occur in a time of the order of a few hundred years or less. □

1. Grootes, P. M., Stuiver, M., White, J. W. C., Johnsen, S. & Jouzel, J. Comparison of oxygen isotope records from GISP2 and GRIP Greenland ice cores. *Nature* **366**, 552–554 (1993).
2. GRIP Climate instability during the last interglacial period recorded in the GRIP ice core. *Nature* **364**, 203–207 (1993).
3. Cortijo, E. *et al.* Eemian cooling in the Norwegian Sea and North Atlantic Ocean preceding continental ice growth. *Nature* **372**, 446–449 (1994).
4. McManus, J. F. *et al.* High-resolution climate records from the North Atlantic during the last interglacial. *Nature* **371**, 326–329 (1994).
5. Maslin, M., Sarnthein, M. & Knaack, J.-J. Subtropical Eastern Atlantic climate during the Eemian. *Naturwissenschaften* **83**, 122–126 (1996).
6. Thouveney, N. *et al.* Climate variations in Europe over the past 140 kyr deduced from rock magnetism. *Nature* **371**, 503–506 (1994).
7. Field, M. H., Huntley, B. & Muller, H. Eemian climate fluctuations observed in a European pollen record. *Nature* **371**, 779–783 (1994).
8. Dansgaard, W. *et al.* Evidence of general instability of past climate from a 250-kyr ice-core record. *Nature* **364**, 218–220 (1993).
9. Shackleton, N. J. The last interglacial in the marine and terrestrial records. *Proc. R. Soc. Lond. B* **174**, 135–154 (1969).
10. Alley, R. B. *et al.* Comparison of deep ice cores. *Nature* **373**, 393–394 (1995).
11. Fuchs, A. & Leuenberger, M. C. δ^{18}O of atmospheric oxygen measured on the GRIP ice core document stratigraphic disturbances in the lowest 10% of the core. *Geophys. Res. Lett.* **23**, 1049–1052 (1996).
12. Keigwin, L. D., Curry, W. B., Lehman, S. J. & Johnsen, S. The role of the deep ocean in North Atlantic climate change between 70 and 130 kyr ago. *Nature* **371**, 323–326 (1994).
13. Oppo, D. W., Horowitz, M. & Lehman, S. Marine core evidence for a sharp decrease in deep water production during Termination II and a relatively stable MIS 5e (Eemian). *Paleoceanography* **12**, 51–64 (1997).
14. Boyle, E. A. & Keigwin, L. D. North Atlantic thermohaline circulation during the last 20,000 years linked to high latitude surface temperature. *Nature* **330**, 35–40 (1987).
15. Shackleton, N. J. & Opdyke, N. D. Oxygen isotope and paleomagnetic stratigraphy of equatorial Pacific core V28-238: oxygen isotope temperatures and ice volumes on 10^6 yr scale. *Quat. Res.* **3**, 39–55 (1973).
16. Schrag, D. P., Hampt, G. & Murry, D. W. Pore fluid constraints on the temperature and oxygen isotopic composition of the Glacial ocean. *Science* **272**, 1930–1932 (1996).
17. Hester, K. & Boyle, E. A. Water chemistry control of cadmium in recent benthic foraminifera. *Nature* **298**, 260–262 (1982).
18. Boyle, E. A. & Keigwin, L. D. Deep circulation of the North Atlantic over the last 200,000 years: geochemical evidence. *Science* **218**, 784–787 (1982).
19. Keigwin, L. D., Jones, G. A., Lehman, S. J. & Boyle, E. A. Deglacial meltwater discharge, North Atlantic deep circulation, and abrupt climate change. *J. Geophys. Res.* **96**, 16811–16826 (1991).
20. Boyle, E. A. Characteristics of the deep ocean carbon system during the past 150,000 years: ΣCO_2 distributions, deep water flow patterns, and abrupt climate change. *Proc. Natl Acad. Sci. USA* **94**, 8300–8307 (1997).
21. Balsam, W. L., Otto-Bliesner, B. L. & Deaton, B. C. Modern and last glacial maximum eolian sedimentation patterns in the Atlantic Ocean interpreted from sediment iron oxide content. *Paleoceanography* **10**, 493–507 (1995).
22. Hollister, C. D. & McCave, I. N. Sedimentation under deep-sea storms. *Nature* **309**, 220–225 (1984).
23. Bacon, M. P. & Rosholt, J. N. Accumulation rates of Th-230, Pa-321, and some transition metals on the Bermuda Rise. *Geochim. Cosmochim. Acta* **46**, 651–666 (1982).
24. Bacon, M. P. Glacial to Interglacial changes in carbonate and clay sedimentation in the Atlantic Ocean estimated from ^{230}Th measurements. *Isotope Geosci.* **2**, 97–111 (1984).
25. Francois, R., Bacon, M. P. & Suman, D. O. ^{230}Th profiling in deep-sea sediments; high-resolution records of changes in flux and dissolution of cabbonate in the equatorial Atlantic during the last 24,000 years. *Paleoceanography* **5**, 761–781 (1990).
26. Martinson, D. G. *et al.* Age dating and the orbital theory of the ice ages: development of high-resolution 0 to 300,000-year chronostratigraphy. *Quat. Res.* **27**, 1–29 (1987).
27. Suman, D. O. & Bacon, M. P. Variations in Holocene sedimentation in the North American basin determined from ^{230}Th measurements. *Deep-Sea Res.* **36**, 869–878 (1989).
28. Laine, E. P. & Hollister, C. D. Geological effects of the Gulf Stream system on the northern Bermuda Rise. *Mar. Geol.* **39**, 277–300 (1981).
29. Belanger, P. E., Curry, W. B. & Matthews, R. K. Core-top evaluation of benthic foraminiferal isotopic ratios for paleo-oceanographic interpretations. *Palaeogeogr. Palaeoclimatol. Palaeoecol.* **33**, 205–220 (1981).
30. Graham, D. W., Corliss, B. H., Bender, M. L. & Keigwin, L. D. Carbon and oxygen isotopic equilibria of recent deep-sea benthic foraminifera. *Mar. Micropaleont.* **6**, 483–497 (1981).
31. Bender, M. *et al.* Climate correlations between Greenland and Antarctica during the past 100,000 years. *Nature* **372**, 663–666 (1994).
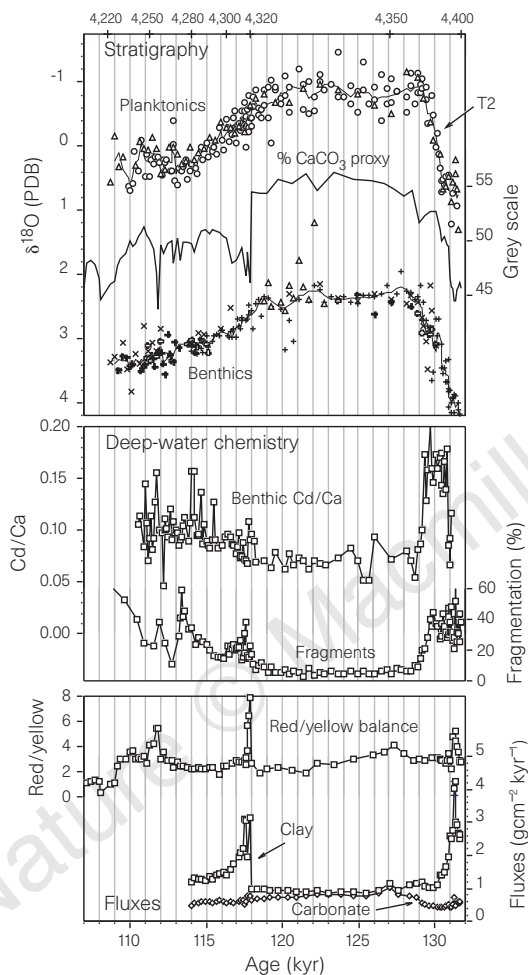
Figure 2 Plots of MD95-2036 data against age and depth. All isotopic data are relative to Pee Dee belemnite (PDB). T2 refers to the position of termination II, the penultimate deglaciation. The symbols in the planktonic stable isotope plot are VG δ^{18}O from *G. ruber* (circles) and Finnigan δ^{18}O from *G. ruber* (triangles). A three-point running average is drawn through the data. Benthic δ^{18}O data are from four sources: VG *Cibicidoides* (upside-down triangles), Finigan *Cibicidoides* (plus signs), *Melonis* (squares) and *Oridorsalis* (circles). The *Melonis* and *Oridorsalis* data were adjusted by −0.35‰ and −0.3‰ respectively to be equivalent to the *Cibicidoides* data. These adjustments are consistent with offsets at depths where the species coexist with *Cibicidoides* and with previous core top studies.[29,30] A *Cibicidoides* equivalent line is drawn through the data as a three-point running average. Cd/Ca ratios are from *N. umbonifera* and are plotted along with the foraminiferal fragmentation index. Carbonate and non-carbonate fluxes from excess ^{230}Th° measurements are plotted with the reflectance red/yellow balance. The age model was calculated from benthic δ^{18}O and ^{230}Th°$_{ex}$ as described in the text. Note that although foraminiferal $MnCO_3$ levels in this deep section of the core are higher than normally considered acceptable (~200 μmol kg^{-1}), the similarity of low-Mn Holocene and stage-5e Cd values suggests that these numbers are not negatively affected at this site.